Advanced XAS Analysis for Investigating Fuel Cell Electrocatalysts

Agnieszka Witkowska[*,†], Emiliano Principi[*], Andrea Di Cicco[*] and Roberto Marassi[**]

[*]*Department of Physics, University of Camerino, Italy*
[†]*Department of Solid State Physics, Gdansk University of Technology, Poland (permanent address)*
[**]*Chemistry Department, University of Camerino, Italy*

Abstract. In the paper we present an accurate structural study of a Pt-based electrode by means of XAS, accounting for both the catalytic nanoparticles size distribution and sample inhomogeneities. Morphology and size distribution of the nanoparticles were investigated by scanning electron microscopy (SEM), transmission electron microscopy (TEM) and X-ray diffraction techniques. XAS data-analysis was performed using advanced multiple-scattering techniques (GNXAS), disentangling possible effects due to surface atom contributions in nanoparticles and sample homogeneity, contributing to a reduction of intensity of the structural signal. This approach for XAS investigation of electrodes of FC devices can represent a viable and reliable way to understand structural details, important for producing more efficient catalytic materials.

Keywords: fuel cell, Pt-based electrode, XAFS
PACS: 82.47.Gh, 61.46.Df, 61.10.Ht,

INTRODUCTION

Today the study of alternative energy sources is one of the main research subject at the world level. Fuel cells (FC) are promising sustainable energy systems which may replace in the long term most current combustion systems in all energy end-use sectors. There are several types of fuel cells which have been studied and have underwent commercial development [1]. One of the most important and universal is the proton exchange membrane fuel cell (PEMFC) [2]. Due to their numerous advantages, PEMFCs are prime candidates for both portable power, automobile, and residential applications.

Many efforts are currently devoted to the study of metallic electrocatalysts in order to improve performances of PEMFCs and to reduce their cost. The size, shape and morphology of the platinum group metal and/or Pt-based metal alloy particles, and the amount and type of adsorbed species on these particles are important physical quantities that directly affect catalyst performance. Therefore, a number of studies have been conducted to characterize the catalyst structure and to understand the chemical properties of the system. In this context, X-ray absorption spectroscopy (XAS) which gives unique information due to its great sensitivity to the local atomic arrangement around the selected catalytic metal site, seems to be a powerful tool [3]. In particular, XAS can be useful for obtaining information on CO poisoning and structural degradation and it can be used "in operando" conditions (in fuel cell-relevant conditions, e.g. [4], or even in a real fuel cell, e.g. [5, 6]).

Nevertheless, to obtain reliable structural information and to avoid misinterpretation XAFS analysis of metallic nanoparticles, unsupported or supported, should be accurate and sophisticated enough.

In this report, we try to focus the readers' attention on some aspects of advanced EXAFS analysis that might influence the values of all strongly inter-correlated structural parameters. Especially, during analysis much attention should be dedicated to the complexity of the nanosystem and sample homogeneity.

EXPERIMENTAL DETAILS

The Pt L_3-edge XAS spectra of two samples of nanocrystalline Pt and of a standard Pt foil were recorded at the BM29 beam-line of the European Synchrotron Radiation Facility, Grenoble, using a double-crystal monochromator equipped with Si(311) crystals.

The two nano-powder Pt samples were: the first, hereafter called Pt1, was an unsupported Pt Black from E-TEK mixed with graphite and pressed into a pellet with a thickness chosen to give optimal jump on the absorption edge, $J \sim 0.8$; the second was a Pt-based electrode for fuel-cells, hereafter called Pt2, EC-20-10-10 from Quintech, Pt loading 1.0 mg/cm^2.

Measurements were performed in the 11.45–12.8 keV energy range under ambient conditions. The sampling procedure was chosen to yield high quality data for both pre- and post-edge background analysis used to normalize the spectra. More details on the experimental setup

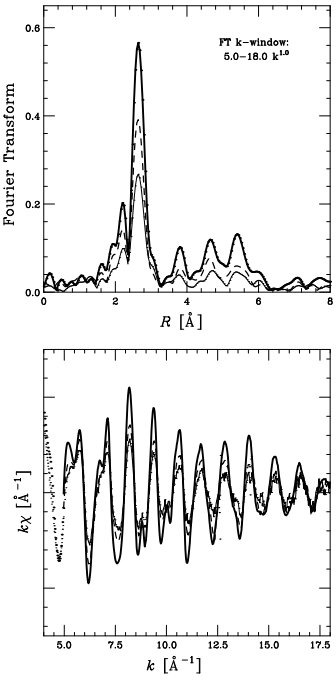

FIGURE 1. Pt L_3-edge EXAFS spectra (after background substraction, k^3 weighted) (bottom) and Fourier Transforms (top) for: Pt-foil – solid thick line, Pt powder – dashed line, Pt-based electrode – solid thin line

can be found in [7].

Because of the systems' complexity detailed morphological and size distribution investigations should be performed before starting EXAFS analysis. We have used scanning electron microscopy (SEM), transmission electron microscopy (TEM) and X-ray diffraction (XRD) measurements to obtain all important micro- and nanoscale information about considered samples, which are essential to understand the differences in XAS signals reported in Figure 1.

SEM analysis of Pt2 surface clearly showed inhomogeneities of the catalytic layer. Many holes and cracks have been observed. From a detailed SEM-image analysis results, that about 10% of whole sample surface was completely free of the catalytic material ($\rho = S_{holes}/S_{tot} \approx 0.1$). A correction of the XAS spectrum, $\alpha = \ln\frac{I_o}{I_1}$, for the observed inhomogeneity can be performed using the following expansion:

$$\alpha = \mu d_o - \rho(e^{\mu d_o} - 1) + \frac{\rho^2}{2}(e^{\mu d_o} - 1)^2 \ldots \qquad (1)$$

The application of this correction has been found to increase the XAS amplitude of about 1%.

TEM-image analysis (200 randomly selected quasi-spherically shaped particles) of Pt1 and Pt2 (catalytic material scraped from the electrode) have been performed to obtain nanoparticle size distributions. The Pt1 distribution is broader and exhibits larger values of the mean Pt crystallite size. A Gaussian function fitting this distribution was found to have a mean particle diameter $D = 4.45 \pm 0.06$nm with standard deviation $\sigma = 0.92 \pm 0.06$nm. For Pt2 we obtained $D = 2.40 \pm 0.05$nm and $\sigma = 0.76 \pm 0.03$nm.

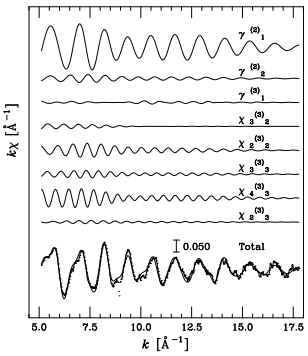

FIGURE 2. The best fit results of GNXAS analysis performed for Pt-based electrode at Pt L_3-edge (k^3 weighted). Upper curves represent components of the model signal: $\gamma^{(2)}$ – total two-body signal for the first and second shells; $\gamma^{(3)}$ – total three-body signal for triangle configuration with angle of 60°; $\chi_4^{(3)}$, $\chi_3^{(3)}$, $\chi_2^{(3)}$ – triple, double and long bond single scattering signals for triangle configurations with angle of 120° and 180°.

The platinum crystal size in Pt1 and Pt2 samples have also been estimated using X-ray diffraction patterns and Scherrer equation (the (111), (200), (220) and (311) peaks have been used). For Pt2, in the error range associated with analysis techniques, the obtained value is consistent with TEM studies. XRD extracted cluster diameter, taking into account relatively narrow size distribution, equals to 2.5 ± 0.3nm. For Pt1 we obtained somewhat overestimated value, $D = 6.4 \pm 1.1$nm, in respect to the TEM result. The latter effect results probably from the increased weight of large particles in the size distribution for Pt1.

EXAFS ANALYSIS

The experimental data were analysed with an advanced technique using theoretical calculations of the X-ray absorption cross-section in the framework of the GNXAS method [8, 9]. GNXAS method allows for a proper inclusion of "ab-initio" multiple scattering (MS) contributions in the EXAFS data-analysis. In our analysis, we have considered all MS contributions up to the fourth shell, as presented in Figure 2. Moreover, during the atomic background modelling the $(2p\,4f)$ and $(2p\,4p)$ two-electron channels have been considered, e.g. [10].

In the case of nano-material analysis much attention

TABLE 1. Structural parameters obtained by GNXAS analysis: R [Å] – the average inter-atomic distance, R_o [Å] – the most probable inter-atomic distance, σ^2 [10^{-3} Å^2] – the standard deviation of distance, β – the skewness parameter, N – the coordination number.

	R	R_o	σ^2	β	N
Pt foil	2.764(2)	2.764	4.6(2)	0.0	12.0(5)
	3.914(8)	3.914	7.0(2)	0.0	6.0(5)
Pt1	2.763(2)	2.756	5.1(3)	0.1(1)	9.2(9)
	3.923(8)	3.907	8.5(5)	0.3(2)	4.0(5)
Pt2	2.767(3)	2.758	6.0(5)	0.1(1)	7.6(8)
	3.93(1)	3.910	7.9(5)	0.3(2)	3.1(3)

should also be dedicated to a strong correlation between the parameters. Therefore, it is very important to find a reliable way to perform a suitable "decorrelation" between them. For example, for N, σ^2 and S_0^2 parameters we use the following procedure. S_0^2 value has been estimated by Pt foil EXAFS data analysis, in which we fixed coordination number values, as for bulk fcc structure, and constrained Debye-Waller factors around values calculated with force-constant models, e.g. [11]. The obtained $S_0^2 = 0.85 \pm 0.1$ value has been applied for all the other nano-material data analysis, in which the Pt foil disorder parameters have been used as lower limits. The size distributions of Pt nanoparticles, with a fcc-like structure (as follows from the XRD analysis) have been used to determine the allowed ranges for coordination numbers.

Furthermore, to take into account anharmonicity effect in our consideration the metal-metal radial distribution was modelled by a Γ-like function [12].

RESULTS AND DISCUSSION

Pt foil, Pt1 and Pt2 EXAFS signals and their Fourier Transforms are shown in Figure 1, while detailed results of GNXAS structural refinements are presented in Table 1. The obtained Pt foil parameters agree well with crystallographic and vibrational data found in the literature. For the nano-materials, the parameters of the two nearest shells have been determined with a reasonable accuracy.

For all the shells, a contraction of the most probable Pt-Pt distances and a reduction (as expected from the presence of a significant fraction of surface atoms) of the coordination numbers in respect to the foil-values have been observed. These contractions are comparable with changes previously found by other authors working with catalytic nano-systems, e.g. [13, 14, 15].

The obtained N values, using simple icosahedral and cuboctahedral models of spherical Pt nano-clusters, are associated with mean particle sizes lower then those measured by TEM and XRD. The most probable explanations of this discrepancy could be as follows: TEM and XRD results overestimate dimension of a mean cluster; observed nanoparticles have not ideally spherical shape; some strain is present in nano-materials. Thus, most sophisticated cluster calculations or modelling are needed to correlate the coordination number reduction and bond length contraction with nanoparticle sizes.

The values of the variance, σ^2, and asymmetry, β, in bond length distributions measure both thermal and static disorder. In order to draw conclusions about the observed increase in σ^2 and β parameters detail temperature-dependent analysis is necessary.

CONCLUSIONS

In the paper we have presented an accurate structural study of a Pt nano-materials on the basis of the GNXAS approach accounting for effects due to surface atom contributions in nanoparticles and sample inhomogeneity. We show some aspects of an advanced EXAFS analysis that might influence the values of structural parameters. The obtained results will be used in our future works on electrodes of operating fuel cells.

REFERENCES

1. J. Larminie and A. Dicks, *Fuel Cell Systems Explained*, Second Edition, J. Wiley and Sons, England, 2003.
2. T.R. Ralph, and M.P. Hogarth, *Platinum Metals Rev.* **46** (1), 3–14 (part I); *ibid.* 117–135 (part II) (2002).
3. A.E. Russell, and A. Rose, *Chem. Rev.* **104**, 4613–4635 (2004).
4. S. Maniquet, R.J. Mathew, and A.E. Russell, *J. Phys. Chem. B* **104**, 1998–2004 (2000).
5. R. Viswanathan et al. *J. Phys. Chem.* **B 106**, 3458–3465 (2002).
6. R.J.K. Wiltshire et al. *Electrochim. Acta* **50**, 5208–5217 (2005).
7. A. Filipponi et al. *Rev. Sci. Instrum.* **71**, 2422–2432 (2000).
8. A. Filipponi, A. Di Cicco, and C.R. Natoli, *Phys. Rev.* **B 52**, 15122–15134 (1995).
9. A. Filipponi, and A. Di Cicco, *Phys. Rev.* **B 52**, 15135–15149 (1995).
10. A. Di Cicco, and A. Filipponi, *Phys. Rev.* **B 49**, 12564–12571 (1994).
11. E. Sevillano, H. Meuth, and J.J. Rehr, *Phys. Rev.* **B 20**, 4908–4911 (1979).
12. A. Di Cicco et al. *J. Phys. CM* **8** 10779–10797 (1996).
13. R.E. Benfield, A. Filipponi, N. Morgante, and G. Schmid, *J. Organomet. Chem.* **573** 299–304 (1999).
14. A.I. Frenkel, Ch.W. Hills, and R.G. Nuzzi, *J. Phys. Chem.* **B 105** (51), 12689–12703 (2001).
15. A.Yu. Stakheev et al. *Russ. Chem. Bull., Int. Ed.* **53** (3), 528–537 (2004).